Research Square

Preprints are preliminary reports that have not undergone peer review.
They should not be considered conclusive, used to inform clinical practice,
or referenced by the media as validated information.

Integrative Pan-Cancer Multi-Omics Analysis Reveals POLQ as a Prognostic Biomarker and Immunotherapeutic Target in Uterine Corpus Endometrial Carcinoma

Bo Du
People's Hospital Affiliated to Shandong First Medical University
Chao Wang
People's Hospital Affiliated to Shandong First Medical University
Yinfeng Lv
People's Hospital Affiliated to Shandong First Medical University
Qun Wang
People's Hospital Affiliated to Shandong First Medical University
Fang Wang
People's Hospital Affiliated to Shandong First Medical University
Jing Li
People's Hospital Affiliated to Shandong First Medical University
He Gao
People's Hospital Affiliated to Shandong First Medical University
Rui Chang
People's Hospital Affiliated to Shandong First Medical University
Hui Li
cklihui@163.com

People's Hospital Affiliated to Shandong First Medical University

Research Article

Keywords: POLQ, pan-cancer, uterine corpus endometrial carcinoma, bioinformatics, immunotherapy, biomarker

Posted Date: November 3rd, 2026

DOI: https://doi.org/10.21203/rs.3.rs-11107769/v1

License: This work is licensed under a Creative Commons Attribution 4.0 International License.
Read Full License

Additional Declarations: No competing interests reported.

Abstract

DNA polymerase theta (POLQ) mediates microhomology-mediated end joining and represents a synthetic lethal target for homologous recombination deficient cancers, yet its pan-cancer clinical, immunoregulatory and predictive functions are poorly defined. Multi-omics data from TCGA, GTEx, cBioPortal, TIMER2.0 and GSCA were used for pan-cancer profiling of POLQ expression, mutations, prognosis, immune signatures. Drug sensitivity correlation analysis together with in silico molecular docking simulations were applied to predict potential binding between POLQ and candidate therapeutic agents. Differential gene expression analysis and functional enrichment were further investigated in uterine corpus endometrial carcinoma (UCEC). POLQ was overexpressed in most malignancies, associated with advanced stages and poor survival. Gene amplification drove its upregulation. POLQ expression showed significant correlations with immune cell infiltration, tumor mutation burden, and microsatellite instability. The strong negative correlations between POLQ expression and responses to multiple chemotherapeutic agents, with molecular docking predicted potential direct interactions between vincristine, paclitaxel, docetaxel and the POLQ protein. In UCEC, high POLQ activated DNA replication, cell cycle and ATR-dependent DNA damage pathways. POLQ is a pan-cancer prognostic and therapeutic biomarker. In UCEC, it accelerates tumor progression via DNA damage and cell cycle dysregulation and reshapes immune microenvironment, supporting POLQ-targeted precision immunotherapy especially for endometrial cancer.

Introduction

Malignancies constitute a major global public health crisis, with continuously rising incidence and mortality rates across all populations. Traditional clinical interventions, such as radical surgery and systemic chemotherapy, frequently yield suboptimal long-term therapeutic effects [1]. While endocrine therapies, molecularly targeted drugs and immune checkpoint inhibitors have refined clinical strategies over the past decades, only a small subset of patients acquire sustained therapeutic responses [2]. Tumorigenesis arises from stepwise accumulation of somatic genetic aberrations, and genome instability acts as a central oncogenic trigger throughout cancer progression [3]. Error-prone DNA repair machinery drives stochastic mutagenesis, conferring tumor cells with adaptive survival advantages under selective pressure within the tumor microenvironment [4]. Defective DNA repair machinery drives the accumulation of genetic lesions, triggering single-strand breaks and lethal DNA double-strand breaks (DSBs) to facilitate tumor initiation and progression [5]. Two high-fidelity pathways maintain genomic integrity via DSB repair: canonical nonhomologous end joining and homologous recombination (HR), while microhomology-mediated end joining (MMEJ) acts as an error-prone backup repair pathway [6]. Advanced tumors frequently develop primary or acquired resistance to PARP inhibitors via diverse adaptive mechanisms, spurring the discovery of novel synthetic lethal targets within DNA repair networks [7].

POLQ (DNA polymerase theta) is a bifunctional low-fidelity enzyme harboring helicase and polymerase activities, functioning as the central mediator of MMEJ-mediated DSB repair [8]. Devoid of 3'-5' exonuclease proofreading activity, POLQ introduces frequent genomic deletions and chromosomal rearrangements, further aggravating genome instability [9]. When HR is impaired—for instance, in BRCA1/2-mutated cancers—cells become critically dependent on POLQ-dependent MMEJ for survival [10]. Pharmacological suppression of POLQ blocks compensatory error-prone repair and triggers synthetic lethality, selectively eliminating HR-deficient tumor cells [11]. Accordingly, POLQ inhibitors have emerged as a promising category of anticancer agents for HR-deficient malignancies [12].

Several pan-cancer bioinformatics analyses of POLQ have been reported [13,14]. POLQ overexpression has been documented in 21 types of malignancies and is consistently associated with poor survival across multiple cancer types [13,14]. Additionally, POLQ mutations have been linked to therapy-induced mutagenesis in advanced tumors [15]. However, most have not systematically examined UCEC-specific immune microenvironment features, chemosensitivity correlates, or in silico drug-target docking. This gap limits the translational utility of POLQ as a biomarker for endometrial cancer.

UCEC is one of the most prevalent gynecologic malignancies with steadily increasing incidence, and advanced or recurrent cases carry extremely poor prognosis [16]. The etiology of endometrial cancer remains unclear to date, and there is a lack of effective treatment methods and prognostic indicators. Immune checkpoint blockade (ICB) provides novel therapeutic options for late-stage UCEC, yet single-agent ICB yields an objective response rate of merely ~ 13%, largely restricted by the absence of reliable predictive biomarkers [17]. Pan-cancer evidence has established tight links between dysregulated DNA damage repair and tumor immunogenicity, supporting the screening of repair-related genes as cross-cancer immunotherapy markers [14]. Aberrant POLQ expression elevates tumor mutational burden and genomic instability; previous pan-cancer reports have documented POLQ overexpression in bladder, pancreatic and multiple other cancers, correlating with ICB response, and combined POLQ inhibition and immunotherapy exerts synergistic antitumor effects [18]. In UCEC, elevated POLQ expression has been linked to unfavorable survival, whereas its immunomodulatory roles and underlying molecular mechanisms remain largely uncharacterized [19].

Herein, we adopted an integrative pan-cancer multi-omics framework to characterize POLQ expression signatures across human malignancies. We further focused on UCEC cohorts to systematically dissect the correlations of POLQ with clinicopathological features, tumor immune microenvironment and therapeutic response, and uncovered its downstream functional pathways. Distinct from previous pan-cancer surveys of POLQ, the present study places additional emphasis on UCEC-specific immune-related signatures, chemotherapeutic response prediction and in silico drug target docking screening. This work aims to identify POLQ as a novel biomarker and actionable therapeutic target to advance precision immunotherapy for endometrial carcinoma.

Materials and Methods

Data Acquisition and Preprocessing

All datasets analyzed in this study were retrieved from publicly accessible databases and web-based bioinformatics tools. RNA-seq profiles from The Cancer Genome Atlas (TCGA) and Genotype-Tissue Expression (GTEx) projects were downloaded from the University of California, Santa Cruz Xena (UCSC Xena) portal (https://xenabrowser.net/datapages/), where raw data were uniformly processed using the Toil pipeline as previously described. Additional resources included cBioPortal (https://www.cbioportal.org), TIMER2.0 (https://compbio.cn/timer2), and GSCA (https://guolab.wchscu.cn/GSCA/#/). Statistical computations and graphical visualizations were conducted via Xiantao Academic (https://www.xiantaozi.com), a web-based bioinformatics analysis toolkit. For drug sensitivity analysis and molecular docking, RCSB PDB (https://www.rcsb.org/), PubChem (https://pubchem.ncbi.nlm.nih.gov/) and CB-Dock2 (http://cao.labshare.cn:11080/cb-dock2/php/index.php) were used for data retrieval and visualization.

For all transcriptome data quantified as transcripts per million (TPM), $\log_2(\text{TPM} + 1)$ transformation was applied for standardized normalization across samples. Specimens with incomplete expression profiles, clinical annotations or auxiliary information were excluded to guarantee data integrity and analytical reliability. Uniform data cleaning, missing value filtering and normalization were implemented for all included datasets.

Pan-cancer Expression Analysis of POLQ

Two independent RNA-seq datasets were utilized to characterize the pan-cancer expression pattern of POLQ. First, TPM-normalized transcriptomic data of TCGA pan-cancer tumor tissues and matched normal tissues from GTEx were extracted. The Mann-Whitney U test (Wilcoxon rank-sum test) was used to compare POLQ expression levels between tumor and normal tissue groups. Second, STAR-processed RNA-seq data from the TCGA pan-cancer cohort were collected, and paired tumor and adjacent non-tumor tissues from identical patients were compared using the Wilcoxon signed-rank test. All expression analyses and visualizations were completed using Xiantao Academic.

Prognostic and Diagnostic Analysis

Integrated pan-cancer transcriptomic and clinical datasets from UCSC Xena were used to assess the prognostic and diagnostic potential of POLQ. Univariate Cox regression and Kaplan-Meier survival analyses were performed to evaluate the associations between POLQ expression and overall survival (OS), progression-free interval (PFI), and disease-specific survival (DSS). Hazard ratios (HR) with 95% confidence intervals (CIs) were computed. Prior to Cox regression modelling, the proportional hazards assumption was verified. Receiver operating characteristic (ROC) curves and the corresponding area under the curve (AUC) were generated to quantify the diagnostic performance of POLQ across diverse cancer types.

Clinicopathological Correlation Analysis

TCGA datasets with complete clinicopathological records were enrolled for this analysis. Solid tumors presenting aberrant POLQ expression and paired normal tissues were included. All samples were stratified according to the AJCC/UICC staging system, including T stage (T1–T4), N stage (N0–N3), M stage (M0, M1), and overall pathological stage (Stage I–IV). Normal tissues were set as the control group. Box plots were generated to illustrate the distribution of POLQ expression across distinct clinicopathological subgroups. The Kruskal-Wallis test followed by Dunn's multiple comparison test with Benjamini-Hochberg P value adjustment was adopted for intergroup comparisons.

Genetic Alteration and Methylation Analysis

Data regarding somatic mutations, protein domain architecture, copy number variation (CNV), DNA methylation and mRNA expression of POLQ across pan-cancer cohorts were acquired from cBioPortal. We systematically analyzed the mutation distribution across functional domains of POLQ and calculated the frequencies of gene mutation, amplification and deletion in individual cancer types.

Immune Landscape Analysis

Immune-related molecular profiles and clinical metadata of multiple common human malignancies were obtained from the TIMER2.0 database, while tumor mutation burden (TMB) and microsatellite instability (MSI) data covering 33 cancer types were extracted from cBioPortal. We further analyzed five major categories of core immune genes, including chemokine receptors, immune checkpoint molecules, costimulatory and coinhibitory molecules, human leukocyte antigen (HLA) and antigen presentation-related genes. Pearson's correlation analysis was applied to calculate pairwise correlation coefficients and heatmaps were generated to visualize expression patterns. Spearman's correlation test was additionally conducted to explore the expression relationships of genes associated with immune activation, immune suppression and inflammatory responses based on the TCGA pan-cancer dataset.

Drug Sensitivity Analysis and Molecular Docking Simulation

Pan-cancer drug sensitivity correlation analysis was performed via the GSCA platform using public Genomics of Drug Sensitivity in Cancer (GDSC) and Cancer Therapeutics Response Portal (CTRP) cell line datasets. Half-maximal inhibitory concentration (IC_{50}) and area under the dose-response curve (AUDRC) quantified cellular drug response, and Spearman correlation tests evaluated associations between POLQ mRNA expression and antitumor agent sensitivity. Statistical significance was defined as FDR ≤ 0.05, with all correlation plots generated by GSCA's built-in visualization tools.

To further validate the direct binding interaction between POLQ and representative screened drugs, molecular docking simulation was subsequently carried out. The 3D crystal structure of the human POLQ protein was retrieved from the RCSB Protein Data Bank under PDB ID 5A9J, which corresponds to the C-

terminal polymerase domain of POLQ resolved at 3.55 Å. Prior to docking, the protein structure was prepared by removing water molecules and bound co-crystallized ligands. The 3D chemical structures of six candidate compounds (vincristine, paclitaxel, docetaxel, 3-Cl-AHPC, methotrexate, and gemcitabine) were downloaded from PubChem in SDF format (Supplementary 1) and energy-minimized using the MMFF94 force field. Blind protein-ligand docking was conducted on the CB-Dock2 server. The docking box was automatically centered on the predicted binding site without manual specification, covering the entire protein surface for blind docking. For each ligand, the top 10 docking poses were generated and ranked by predicted binding affinity (Vina score, kcal/mol); the pose with the lowest binding energy was selected as the optimal conformation for each compound.

Differential Expression and Functional Enrichment in UCEC

Transcriptomic and clinical data of 589 endometrial carcinoma specimens and 35 paired adjacent non-tumor samples were downloaded from TCGA. Samples were divided into POLQ high- and low-expression subgroups based on the median expression level. Differentially expressed genes (DEGs) were screened using the criteria of $|\log_2 FC| > 2.5$ and adjusted $P < 0.05$. A relatively stringent $|\log_2 FC| > 2.5$ cutoff was selected to prioritize genes with large magnitude transcriptional changes for subsequent network and enrichment analyses. A protein-protein interaction (PPI) network was constructed using the identified DEGs. The top 30 highly expressed genes from each subgroup were selected for co-expression analysis to uncover transcriptional regulatory patterns. Gene Set Enrichment Analysis (GSEA) was performed to clarify the biological functions and signaling pathways modulated by these DEGs, using the Molecular Signatures Database (MSigDB) hallmark gene set collection and curated gene sets, with FDR < 0.25 considered significantly enriched.

Clinical Relevance Analysis in UCEC

After excluding normal tissues and samples with missing clinical information, a total of 554 UCEC samples with complete RNA-seq data and clinical records were included in this section. Transcriptomic data were normalized via $\log_2(\text{value} + 1)$ transformation. The Cox proportional hazards regression model was built using R 4.2.1 along with the survival and rms packages, with overall survival set as the primary clinical endpoint. Univariate Cox regression analysis was conducted with a screening cutoff of $P = 0.1$ to evaluate the correlations of patient prognosis with POLQ expression, tumor stage, histological grade, patient age and other clinical indicators. The Shapiro-Wilk test and Levene's test were used to assess data normality and homogeneity of variance. For datasets that failed to satisfy these two assumptions, the Kruskal-Wallis test combined with Dunn's multiple comparison test was used to compare POLQ expression across different histological grades. Valid outliers confirmed to be non-artifactual were retained in subsequent analyses.

Results

Pan-Cancer Expression Patterns of POLQ

We first analyzed POLQ mRNA expression across 33 cancer types and corresponding normal tissues from the TCGA and GTEx databases. Analysis of POLQ mRNA expression across 33 cancer types revealed that POLQ was expressed at extremely low levels in normal tissues of multiple cancer types, including kidney chromophobe (KICH), kidney renal clear cell carcinoma (KIRC), kidney renal papillary cell carcinoma (KIRP), acute myeloid leukemia (LAML) and glioblastoma multiforme (GBM), while its expression was markedly upregulated in the matched tumor tissues (Fig. 1A). No significant expression difference was observed between tumor and normal tissues in thyroid carcinoma (THCA) ($P = 0.087$, Wilcoxon rank-sum test, not significant). For cholangiocarcinoma (CHOL), the limited number of available normal tissue samples precluded robust estimation of baseline POLQ expression in non-neoplastic biliary tissue. Notably, POLQ expression was significantly higher in tumor tissues than in normal counterparts in cervical squamous cell carcinoma and endocervical adenocarcinoma (CESC), LAML and diffuse large B-cell lymphoma (DLBC).

Prognostic and Diagnostic Performance of POLQ

Univariate survival analyses were conducted to evaluate the correlation between POLQ expression and three key clinical endpoints, including OS, DSS and PFI across pan-cancer cohorts. Hazard ratio and 95% confidence interval (CI) were used to assess prognostic risk, where a Hazard ratio > 1 indicated an unfavorable prognostic factor and a Hazard ratio < 1 represented a protective factor.

Forest plots revealed that elevated POLQ expression was associated with shorter OS in adrenocortical carcinoma (ACC), KIRC, KIRP, brain lower grade glioma (LGG), liver hepatocellular carcinoma (LIHC), lung adenocarcinoma (LUAD), mesothelioma (MESO), PAAD and UCEC (Fig. 2A). The DSS results were highly consistent with the OS outcomes (Fig. 2B). For PFI (Fig. 2C), the list of cancer types with poor prognosis related to high POLQ expression additionally included KICH, prostate adenocarcinoma (PRAD), sarcoma (SARC) and THCA.

ROC curve analysis was applied to assess the diagnostic capacity of POLQ. The AUC values exceeded 0.9 in UCEC, bladder urothelial carcinoma (BLCA), colon adenocarcinoma (COAD), GBM, lung squamous cell carcinoma (LUSC), ovarian serous cystadenocarcinoma (OV), stomach adenocarcinoma (STAD) and PAAD (Figs. 2D, 2E), demonstrating the excellent diagnostic efficacy of POLQ in these malignancies. Overall, POLQ exhibited distinct tumor-specific heterogeneity in prognostic roles. High POLQ expression was an independent risk factor for inferior OS, DSS and PFI in ACC, KIRC, KIRP, LGG, LIHC, LUAD, MESO, PAAD and UCEC. Conversely, increased POLQ expression acted as a protective factor in a small number of cancers such as gastric cancer and thymoma. No significant correlation was detected in most remaining cancer types.

Correlation with Clinicopathological Staging and Grading

We systematically explored POLQ expression profiles in normal tissues and tumor samples stratified by T stage (Figs. 3A), N stage (Figs. 3B), M stage (Figs. 3C), and overall pathological stage (Figs. 3D), across ten common cancers, namely BLCA, breast invasive carcinoma (BRCA), COAD, esophageal carcinoma (ESCA), head and neck squamous cell carcinoma (HNSC), LIHC, LUAD, LUSC, rectum adenocarcinoma (READ) and STAD.

POLQ maintained low basal expression in all normal tissues and was universally upregulated in tumor tissues. With the progression of clinicopathological characteristics, POLQ expression displayed a gradual increasing trend. Specifically, elevated tumor invasion depth (T1 to T4), aggravated lymph node metastasis (N0 to N3), distant metastasis (M0 to M1) and advanced overall pathological stage (Stage I–II to Stage III–IV) were accompanied by higher POLQ levels. Tumors at T3–T4 stage, N2–N3 stage, M1 stage and Stage III–IV showed significantly higher POLQ expression than normal tissues and early-stage tumors without metastasis.

All ten enrolled cancers presented identical expression trends. These results confirm that aberrant upregulation of POLQ is closely linked to local invasion, lymph node metastasis, distant metastasis and malignant progression of tumors, indicating that POLQ can be used as a potential molecular indicator for evaluating clinicopathological progression and tumor stage.

Genetic Alterations of POLQ in Pan-Cancer Cohorts

The genetic alteration landscape of POLQ across pan-cancer cohorts was characterized using cBioPortal data. The overall alteration frequency varied substantially by cancer type, with the highest rates observed in non-small cell lung cancer, endometrial carcinoma, and bladder cancer, primarily driven by amplification events (Fig. 4A). A lollipop plot mapping mutations to the POLQ protein sequence showed that variants, including missense and truncating mutations, were distributed across the entire coding region, with a notable hotspot at the C-terminal DNA polymerase domain and a recurrent truncating mutation at Q1361 (Fig. 4B). CNV analysis revealed that amplification was the most frequent event in high-expression tumors, while deep deletions were rare (Fig. 4C). Stratification by CNV status demonstrated a positive correlation between copy number and POLQ mRNA expression, with amplified samples showing significantly higher expression (Fig. 4D). The oncoprint visualization further highlighted inter-patient heterogeneity, with amplification as the dominant alteration type (Fig. 4E).

Pan-Cancer Immune Cell Infiltration

Based on the immune profiles retrieved from the TIMER2.0 database, we systematically evaluated the landscape of immune cell infiltration and immune signatures across multiple human malignancies (Fig. 5). Distinct heterogeneity in immune phenotypes was observed among different cancer types. Cancers including BLCA, CESC, ESCA, STAD, HNSC, skin cutaneous melanoma (SKCM), LUAD, LUSC, uterine carcinosarcoma (UCS) and UCEC were characterized by high immunogenicity and abundant immune cell infiltration. In contrast, ACC, BRCA, CHOL, COAD, DLBC, GBM, LGG, KICH, KIRC, KIRP, LAML, LIHC, MESO, OV, PAAD, PRAD, READ and THCA exhibited low immune scores and limited immune cell

infiltration. Statistical analysis confirmed significant differences in immune-related indicators between the above two groups of cancers.

Tumor Mutation Burden and Microsatellite Instability

TMB (Fig. 6A) and MSI (Fig. 6B) displayed prominent heterogeneity across cancer types. Cancers with high TMB and high MSI included SKCM, LUAD, LUSC, HNSC, ESCA, STAD, BLCA, UCEC, CESC and UCS. By comparison, ACC, uveal melanoma (UVM), BRCA, thymoma (THYM), CHOL, THCA, COAD, testicular germ cell tumors (TGCT), DLBC, GBM, SARC, READ, KICH, PRAD, KIRC, PCPG, KIRP, PAAD, LAML, OV, LGG, LIHC and MESO were characterized by low TMB and low MSI. Radar plots were generated to visualize the distribution of TMB and MSI across pan-cancer cohorts, and significant intergroup differences were observed.

Expression Correlation of Immune-Related Molecules

We systematically analyzed the expression correlations of five categories of core immune genes across pan-cancer cohorts, including immune suppressor genes, immune activator genes, major histocompatibility complex (MHC) genes, inflammatory factor genes and inflammatory receptor genes (Fig. 7A–7E). The analyzed gene sets contained immune checkpoint molecules, costimulatory and coinhibitory molecules, HLA family members, antigen presentation-related genes, chemokines and chemokine receptors. Pearson's correlation analysis was performed to calculate pairwise correlation coefficients among these genes, and Spearman's correlation test was further applied to assess the expression relationships of genes associated with immune activation, immune suppression and inflammatory responses based on the TCGA pan-cancer dataset.

Distinct cancer-specific expression patterns and modular clustering characteristics were observed among immune-related genes. Strong positive or negative correlations (defined as $|r| > 0.6$, Spearman's correlation) were detected in SKCM, HNSC, COAD, LUSC, DLBC, STAD and OV. In contrast, relatively weak overall correlations ($|r| < 0.3$) were found in THCA, LAML, PCPG, PAAD and GBM. Genes belonging to the same functional family exhibited synergistic expression trends across most cancer types.

Drug Sensitivity and Molecular Docking

Pan-cancer correlation analysis filtered by FDR ≤ 0.05 revealed consistent trends across GDSC and CTRP cohorts retrieved from GSCA. In GDSC (Fig. 8A), POLQ expression correlated significantly with over 30 targeted and chemotherapeutic agents; most compounds exhibited negative correlations, and all −Log10(FDR) values ranged from 9.7 to 9.9, indicating highly robust statistical signals. In CTRP (Fig. 8B), POLQ mRNA levels showed widespread negative correlations with common clinical chemotherapies, with −Log10(FDR) values between 9.2 and 9.8, demonstrating higher POLQ expression generally predicted enhanced drug sensitivity across cancer cell lines. Molecular docking further predicted the binding capacity of these clinical agents to POLQ protein. Docking results (Fig. 8C) showed favorable predicted binding affinity between POLQ and all six tested compounds, with vincristine showing the

strongest predicted binding (Vina score = − 12.1 kcal/mol), followed by 3-Cl-AHPC (− 10.7 kcal/mol), paclitaxel (− 10.5 kcal/mol), docetaxel (− 10.0 kcal/mol), methotrexate (− 9.8 kcal/mol), and gemcitabine with the weakest affinity (− 7.1 kcal/mol). Pan-cancer survival and differential expression results further validated that elevated POLQ expression correlates with worse overall survival and advanced histologic grades across multiple tumor types.

Differential Gene Expression and Functional Enrichment in UCEC

Based on the expression level of POLQ, all UCEC samples were divided into high-expression and low-expression groups to screen differentially expressed genes (DEGs). A volcano plot was generated to present the overall distribution of DEGs (Fig. 9A). Obvious expression divergence was observed between the two subgroups: genes of the MAGE family and CT45A1 were markedly upregulated, while members of the DEFA and KLK families were significantly downregulated.

We further constructed two co-expression heatmaps to visualize the expression patterns of the top 30 upregulated and top 30 downregulated DEGs (Fig. 9B, 9C). The results revealed strong synergistic expression trends among genes within each subgroup. A protein-protein interaction (PPI) network was subsequently built using 64 qualified DEGs, which uncovered intricate regulatory interactions among these molecules (Fig. 9D).

Gene Set Enrichment Analysis (GSEA) was performed to explore functional characteristics of DEGs. The GSEA ridge plot displayed the overall enrichment landscape of multiple pathways (Fig. 9E), while advanced visualization plots further confirmed that these DEGs were predominantly enriched in cell cycle, DNA replication, ATR-mediated DNA damage response and mitotic spindle checkpoint pathways (Fig. 9F). Pathway correlation analysis via the GSCA database further verified the close relationships between POLQ expression and multiple oncogenic signaling cascades in UCEC, such as DNA damage response, cell cycle, epithelial-mesenchymal transition (EMT), PI3K-AKT and RAS-MAPK pathways (Fig. 9G).

Consistent with the enrichment results, aberrant POLQ expression was tightly linked to the activation of DNA damage response and cell cycle dysregulation. Additionally, altered POLQ expression profoundly remodeled the abundance of infiltrating immune cells in the UCEC tumor microenvironment. These findings collectively provide solid functional evidence supporting the involvement of POLQ in tumorigenesis, signal transduction and immune regulation of endometrial carcinoma.

Discussion

In normal human tissues, POLQ is highly expressed in bone marrow, thymus, splenic B cells, and germinal centers, with the highest expression levels observed in testicular tissue, but hardly expressed in heart, liver, lung, kidney, brain, spinal cord and small intestine [16]. Elevated expression of POLQ has been

observed across multiple human malignancies, encompassing prostate, hepatocellular, colorectal, and pancreatic carcinomas [21,22,23,13,24]. Upregulation of POLQ in pan-cancer defines its oncogenic properties and potential as a clinical biomarker.

In this study, we performed a comprehensive pan-cancer multi-omics characterization of POLQ, revealing its widespread overexpression across human malignancies, its prognostic and diagnostic value, its correlation with immune infiltration and genomic instability, and its potential as a predictive biomarker for drug sensitivity. Distinct from previous pan-cancer surveys of POLQ, the present study places additional emphasis on UCEC-specific immune-related signatures, chemotherapeutic response prediction, and in silico drug-target docking screening. We further focused on UCEC to elucidate the functional pathways and immune modulatory roles of POLQ in endometrial carcinoma.

Our findings demonstrate that POLQ is significantly overexpressed in the majority of cancers, with the most pronounced upregulation observed in BLCA, BRCA, LIHC, lung cancer, and UCEC. This broad overexpression pattern underscores the potential centrality of POLQ-mediated MMEJ in cancer cell survival, particularly in tumors with high replication stress or defective HR. Previous studies have established that POLQ is critical for repairing DNA lesions in BRCA-deficient cells [9,10]. Our pan-cancer data extend these observations by showing that POLQ overexpression correlates with advanced clinicopathological features, including deeper tumor invasion, lymph node metastasis, and distant metastasis. This suggests that POLQ may not only serve as a survival factor but also actively contribute to malignant progression.

Survival forest plots demonstrated that high POLQ expression independently predicts inferior OS, DSS and PFI across multiple cancers including ACC, KIRC, LIHC, LUAD, PAAD and UCEC, whereas it acts as a protective factor in a small subset of tumors such as gastric cancer and thymoma. Such tumor-type heterogeneity reflects context-dependent DNA repair network rewiring in distinct tumor genetic backgrounds. Meanwhile, ROC curves yielded AUC values exceeding 0.9 in UCEC, BLCA, COAD, PAAD and other malignancies, strongly supporting POLQ as a high-performance diagnostic marker for tumor screening. Prior research has reported POLQ dysregulation in individual cancer subtypes [16,21,22,23,13,24]; our cross-cancer profiling unifies and extends these observations, establishing POLQ as a pan-cancer oncogenic signature closely linked to tumor progression.

Mutations are thought to be associated with aging, carcinogenesis, and human genetic diseases, and DNA damage is the primary cause of mutations [26,27]. Genetic alteration analysis further revealed POLQ amplification as the dominant genomic event across pan-cancer cohorts, with copy number gain positively correlated with its mRNA abundance. Missense and truncating mutations spread throughout the full-length coding sequence, with a prominent hotspot at the C-terminal DNA polymerase domain. This evidence explains the transcriptional upregulation of POLQ in tumors at the genomic level, supplementing the regulatory mechanism underlying its overexpression beyond transcriptional activation alone.

Genomic instability driven by abnormal DNA repair is a well-established inducer of tumor immunogenicity [27]. Here, we systematically illustrated the close linkage between POLQ expression, TMB, MSI and immune cell infiltration across all cancer types. A particularly notable finding is the strong correlation between POLQ expression and immune-related parameters. Tumors with high POLQ expression generally exhibited elevated TMB and MSI status, accompanied by abundant infiltration of anti-tumor immune cells, including SKCM, HNSC, UCEC and BLCA. In contrast, cancers with low POLQ abundance displayed cold immune phenotypes with limited immune cell recruitment. The significant correlations with TMB and MSI suggest that POLQ-mediated genomic instability may enhance tumor neoantigen load, potentially sensitizing tumors to immune checkpoint blockade. This is consistent with the established role of DNA damage repair defects in enhancing tumor immunogenicity [18]. It should be emphasized that these are correlational observations derived from transcriptome-level data; causal relationships cannot be concluded. Functional experimental work is required to verify whether elevated POLQ directly triggers genomic instability accumulation and subsequent immune microenvironment reprogramming.

Correlation analysis of five core immune gene families further confirmed that POLQ expression positively correlates with antigen presentation molecules (HLA family), immune co-stimulatory factors and multiple immune checkpoint genes. Mechanistically, POLQ-mediated error-prone MMEJ accumulates somatic mutations to generate abundant neoantigens, which facilitate antigen presentation and activate tumor-infiltrating lymphocytes [22]. This provides a critical molecular basis for the association between POLQ and immunotherapy responsiveness. Notably, existing preclinical studies confirmed that POLQ inhibitors combined with immune checkpoint blockade exert synergistic anti-tumor effects [2]; our pan-cancer correlation data further validate this combination strategy from a translational bioinformatics perspective.

GSCA database screening based on GDSC and CTRP cell line datasets consistently revealed widespread negative correlations between POLQ expression and IC_{50} values of multiple chemotherapeutic agents, indicating that tumors with high POLQ expression are more sensitive to chemotherapy. This relationship can be understood through the concept of "repair dependency": as POLQ repairs DNA damage induced by chemotherapeutic drugs, highly expressed POLQ renders tumor cells more dependent on this compensatory repair pathway, thus conferring enhanced drug vulnerability. When POLQ function is suppressed, damaged DNA cannot be efficiently restored, leading to synthetic lethal cell death [9]. Thus, high POLQ expression marks a state of POLQ dependency, which paradoxically confers enhanced vulnerability to POLQ inhibition.

Subsequent blind molecular docking using CB-Dock2 predicted stable binding between POLQ protein and six candidate compounds, with vincristine showing the strongest predicted binding affinity. These in silico docking results provide structural evidence suggesting POLQ as a potential molecular target of conventional chemotherapeutics. Collectively, drug sensitivity analysis and molecular docking jointly demonstrate the dual value of POLQ: it can not only predict chemotherapeutic response for

individualized treatment stratification, but also act as a target for developing novel small-molecule inhibitors to boost anti-tumor efficacy.

UCEC was selected as the representative tumor for in-depth functional validation given its high POLQ expression, excellent diagnostic AUC and significant adverse prognostic hazard ratio. By grouping UCEC samples according to POLQ expression levels, we identified robust DEGs between high- and low-expression subgroups, with tumor antigen genes (MAGE, CT45A1) significantly upregulated and epithelial differentiation-related genes (DEFA, KLK families) markedly suppressed. PPI network construction highlighted tight regulatory interactions among these DEGs, implying that POLQ extensively remodels the transcriptional landscape of endometrial cancer cells.

GSEA results demonstrated that DEGs regulated by POLQ are primarily enriched in cell cycle progression, ATR-dependent DNA damage response, mitotic spindle checkpoint and DNA replication pathways. Additional pathway correlation analysis confirmed strong associations between POLQ and EMT (epithelial-mesenchymal transition), PI3K-AKT as well as RAS-MAPK oncogenic cascades. These results clarify the downstream signaling networks through which POLQ facilitates UCEC malignant phenotypes including proliferation, invasion and metastasis. Nevertheless, our transcriptomic analysis cannot distinguish whether POLQ acts as a primary driver or merely as a downstream correlative marker of these perturbed pathways. Consistent with our pan-cancer immune findings, POLQ overexpression is associated with remodeling of the UCEC immune microenvironment, linking its DNA repair function to tumor immunity in gynecologic malignancies.

In the UCEC tumor microenvironment, POLQ overexpression correlated positively with infiltration of CD8 + T cells and activated memory CD4 + T cells, while showing negative associations with M2-type tumor-associated macrophages. This immune infiltration pattern—characterized by enhanced antigen presentation capacity and reduced immunosuppressive myeloid populations—may partly explain the prognostic impact of POLQ in endometrial cancer and provides a rationale for exploring POLQ as a companion biomarker for ICB response in this malignancy.

A notable genomic interaction involves POLE mutations. Approximately 36% of endometrial cancers with POLE mutations also harbor POLQ mutations. Tumors carrying concurrent POLE and POLQ alterations exhibit significantly higher mutational burden but paradoxically demonstrate 100% disease-free survival, even when POLE mutations occur outside the exonuclease domain. This observation suggests that POLQ status may modify the prognostic landscape of POLE-mutant endometrial cancers, raising the possibility that POLQ could serve as a secondary stratification marker within this molecular subtype. The mechanistic basis for this favorable outcome—whether it reflects enhanced immunogenicity from elevated neoantigen load or distinct DNA repair dynamics—deserves dedicated experimental investigation.

Clinically, late-stage and recurrent UCEC suffers from limited objective response rates to single-agent ICB due to the lack of effective predictive biomarkers [17]. Our data suggest POLQ could serve as a novel

stratification marker to screen UCEC patients suitable for immunotherapy or POLQ inhibitor combination regimens, offering promising translational value for precision treatment of endometrial carcinoma.

Several limitations of this study should be acknowledged. First, all analyses rely entirely on public multi-omics datasets; prospective clinical cohorts and in vitro/in vivo cellular and animal experiments are required to externally validate the diagnostic, prognostic and therapeutic predictive value of POLQ. Second, although molecular docking predicted direct binding between candidate drugs and POLQ, biochemical co-immunoprecipitation and cellular drug intervention assays are needed to confirm the regulatory interaction. Third, the exact upstream transcriptional or epigenetic mechanisms driving POLQ overexpression in UCEC and other tumors remain unexplored in the current work.

Future research directions will focus on three aspects: (1) Performing cellular functional experiments to clarify how POLQ modulates cell cycle, DNA damage repair and immune crosstalk in UCEC; (2) Validating the predictive efficacy of POLQ for immunotherapy and chemotherapy in independent clinical UCEC cohorts; (3) Exploring the anti-tumor synergistic effect of POLQ inhibitors combined with immune checkpoint agents or conventional chemotherapies to advance novel combination therapeutic strategies for HR-deficient tumors. (4) Investigating the mechanistic basis for the favorable prognosis observed in POLQ-mutant/POLE-mutant endometrial cancers, and determining whether POLQ expression levels can further stratify outcomes within POLE-mutant tumors.

Conclusions

In summary, this integrative pan-cancer multi-omics study systematically delineates the expression, genomic alteration, clinical, immunological and therapeutic characteristics of POLQ across human malignancies. POLQ acts as a pan-cancer oncogenic biomarker with reliable diagnostic and prognostic capacity, is associated with tumor immune microenvironment remodeling, and predicts chemotherapeutic sensitivity. Mechanistic exploration in UCEC further suggests that POLQ is associated with activation of cell cycle, DNA damage response and core oncogenic signaling pathways, indicating its potential role in malignant progression. This work provides comprehensive bioinformatics evidence supporting POLQ as a promising biomarker and actionable therapeutic target for precision oncology, especially for individualized management of endometrial carcinoma.

Declarations

Data Availability Statement

All datasets used in this study are publicly available from the following public repositories. RNA-seq profiles and clinical data from The Cancer Genome Atlas (TCGA) and Genotype-Tissue Expression (GTEx) were downloaded from the UCSC Xena portal (https://xenabrowser.net/datapages/). Somatic mutation, protein domain architecture, copy number variation, DNA methylation, mRNA expression,

tumor mutation burden and microsatellite instability data were retrieved from cBioPortal (https://www.cbioportal.org). Immune-related molecular profiles and clinical metadata were obtained from TIMER2.0 (https://compbio.cn/timer2). Gene set enrichment, pathway correlation and drug sensitivity analyses were performed using GSCA (https://guolab.wchscu.cn/GSCA/#/drug), with drug sensitivity data derived from the GDSC and CTRP cell line datasets. Protein structure data were obtained from RCSB PDB (https://www.rcsb.org/structure/5A9J). Chemical structures of candidate compounds were downloaded from PubChem (https://pubchem.ncbi.nlm.nih.gov/). PubChem is temporarily unavailable (HTTP 503). For reproducibility, we can provide the 3D chemical structures of six candidate compounds (vincristine, paclitaxel, docetaxel, 3 Cl AHPC, methotrexate, and gemcitabine) in SDF format in the Supplementary material. Molecular docking was performed using CB-Dock2 (http://cao.labshare.cn:11080/cb-dock2/php/index.php). MSigDB (https://www.gsea-msigdb.org/gsea/msigdb). All data generated or analyzed during this study are included in this published article.

Author Contributions

B.D. and H.L. conceived and designed the study. B.D., C.W., Y.L., Q.W., F.W., J.L., H.G., R.C., and H.L. wrote the original draft. B.D. and H.L. reviewed and edited the manuscript. B.D., C.W., and H.L. performed the formal analysis. B.D., C.W., J.L., and H.L. performed the investigation. B.D. and H.L. contributed to the methodology. Q.W., F.W., and H.L. provided resources. Q.W., H.G., and H.L. performed data curation. B.D. and Q.W. developed the software. B.D., C.W., and H.L. performed validation. B.D. performed visualization. H.L. acquired funding and administered the project. All authors read and approved the final manuscript.

Funding

This work was funded by the “Climbing Peaks, Scaling Mountains and Crossing Ridges” project of the Obstetrics Department of Jinan People's Hospital.

Acknowledgements

We thank DeepSeek for English language editing assistance.

Clinical trial number

Not applicable.

Ethical Approval and Accordance:

The study did not involve human participants, human tissues, or animals. The work was conducted entirely using publicly available, de-identified database datasets and established in vitro cell line models, and therefore falls under research that does not require formal ethics committee approval and written informed consent were not applicable.

Consent to participate

Not applicable.

Consent to publish

Not applicable. All data used in this work are publicly available, and no individual person`s identifiable information is presented. All authors confirm that this manuscript has not been published elsewhere, is not under consideration for publication in any other journal, and that its publication has been approved by all co-authors as well as the responsible authorities at the institutions where the work was carried out.

References

1. Tang PM, Xian YF, Zhang D. Special issue Advances in targeted cancer therapy and mechanisms of resistance-2nd edition. Int J Mol Sci. 2025;26(15):7173. 10.3390/ijms26157173.
2. Caracciolo D, Riillo C, Di Martino MT, Tagliaferri P, Tassone P. Alternative non-homologous end-joining: error-prone DNA repair as cancer's Achilles' heel. Cancers (Basel). 2021;13(6):1392. 10.3390/cancers13061392.
3. Yap TA, Manning HC, Sapra P, Mills GB, O'Connor MJ. Targeting genomic instability in cancer. Cell. 2026;189(8):2278–306. 10.1016/j.cell.2026.03.035.
4. Anderson CJ, Talmane L, Luft J, et al. Strand-resolved mutagenicity of DNA damage and repair. Nature. 2024;630(8017):744–51. 10.1038/s41586-024-07490-1.
5. Zhu M, Wang C, Song D. Dynamic crosstalk between amino acid metabolism and cancer drug efficacy: from mechanisms to therapeutic opportunities. iScience. 2025;28(8):112405. 10.1016/j.isci.2025.112405.
6. Huang J, Cook DE. The contribution of DNA repair pathways to genome editing and evolution in filamentous pathogens. FEMS Microbiol Rev. 2022;46(6):fuac035. 10.1093/femsre/fuac035.
7. Ngoi NYL, Westin SN, Yap TA. Targeting the DNA damage response beyond poly(ADP-ribose) polymerase inhibitors: novel agents and rational combinations. Curr Opin Oncol. 2022;34(5):559–69. 10.1097/CCO.0000000000000867.
8. Thomas C, Avalos-Irving L, Victorino J, et al. Melanoma-derived DNA polymerase theta variants exhibit altered DNA polymerase activity. Biochemistry. 2024;63(9):1107–17. 10.1021/acs.biochem.3c00670.
9. Belan O, Sebald M, Adamowicz M, et al. POLQ seals post-replicative ssDNA gaps to maintain genome stability in BRCA-deficient cancer cells. Mol Cell. 2022;82(24):4664–e46809. 10.1016/j.molcel.2022.11.008.
10. Krais JJ, Glass DJ, Chudoba I, et al. Genetic separation of BRCA1 functions reveal mutation-dependent Polθ vulnerabilities. Nat Commun. 2023;14(1):7714. 10.1038/s41467-023-43446-1.
11. Bazan Russo TD, Mujacic C, Di Giovanni E, et al. Polθ: emerging synthetic lethal partner in homologous recombination-deficient tumors. Cancer Gene Ther. 2024;31(11):1619–31.

10.1038/s41417-024-00815-2.

12. Campanharo CV, Dos Santos Silveira LV, Meira DD, et al. Pan-cancer and multiomics: advanced strategies for diagnosis, prognosis, and therapy in the complex genetic and molecular universe of cancer. Clin Transl Oncol. 2025;27(12):2936–54. 10.1007/s12094-024-03819-4.
13. Yao Q, Gao S, Sun Q, Wang L, Ren J, Wang D. POLQ knockdown inhibits proliferation, migration, and invasion by inducing cell cycle arrest in colorectal cancer. Discov Oncol. 2024;15(1):633. 10.1007/s12672-024-01496-x.
14. Li Z, et al. Systematic analysis of DNA polymerases as therapeutic targets in pan-cancers. BIOCELL. 2024;48(1):123–38. 10.32604/biocell.2023.031568.
15. Pleasance E, et al. Pan-cancer analysis of advanced patient tumors reveals interactions between therapy and genomic landscapes. Nat Cancer. 2020;1:452–68. 10.1038/s43018-020-0050-6.
16. Kawamura K, Bahar R, Seimiya M, et al. DNA polymerase theta is preferentially expressed in lymphoid tissues and upregulated in human cancers. Int J Cancer. 2004;109(1):9–16. 10.1002/ijc.11666.
17. Peng H, He X, Wang Q. Immune checkpoint blockades in gynecological cancers: a review of clinical trials. Acta Obstet Gynecol Scand. 2022;101(9):941–51. 10.1111/aogs.14321.
18. Xie D, Jiang B, Wang S, Wang Q, Wu G. The mechanism and clinical application of DNA damage repair inhibitors combined with immune checkpoint inhibitors in the treatment of urologic cancer. Front Cell Dev Biol. 2023;11:1200466. 10.3389/fcell.2023.1200466.
19. Zhu N, Wang J, Zhang X, Tang K, Gong L, Hu Y. POLQ promotes tumor progression and immunosuppression via ATMP53 signaling in endometrial cancer. Oncol Rep. 2026;55(5):92. 10.3892/or.2026.9097.
20. Liu G, Jin K, Liu Z, et al. POLQ identifies a better response subset to immunotherapy in muscle-invasive bladder cancer with high PD-L1. Cancer Med. 2024;13(12):e6962. 10.1002/cam4.6962.
21. Ravindran F, Jain A, Desai S, et al. Whole-exome sequencing of Indian prostate cancer reveals a novel therapeutic target: POLQ. J Cancer Res Clin Oncol. 2023;149(5):2451–62. 10.1007/s00432-022-04111-0.
22. Pan Q, Wang L, Liu Y, et al. Knockdown of POLQ interferes the development and progression of hepatocellular carcinoma through regulating cell proliferation, apoptosis and migration. Cancer Cell Int. 2021;21(1):482. 10.1186/s12935-021-02178-2.
23. Xu N, Zhang DF, Shi XX, et al. Identification and targeting of POLQ-associated hereditary colorectal cancer. Clin Cancer Res. 2025;31(15):3215–28. 10.1158/1078-0432.CCR-25-0379.
24. Del Puerto Nevado L, Fernández Aceñero MJ, Cebrián A, et al. POLQ immunostaining behaves as a prognostic factor for pancreatic carcinoma. Front Oncol. 2024;14:1433179. 10.3389/fonc.2024.1433179.
25. Rosendahl Huber A, Van Hoeck A, Van Boxtel R. The mutagenic impact of environmental exposures in human cells and cancer: imprints through time. Front Genet. 2021;12:760039. 10.3389/fgene.2021.760039.

26. Kunz BA, Straffon AF, Vonarx EJ. DNA damage-induced mutation: tolerance via translesion synthesis. Mutat Res. 2000;451(1–2):169–85. 10.1016/S0027-5107(00)00067-6.
27. Xu Y, Nowsheen S, Deng M. DNA repair deficiency regulates immunity response in cancers: molecular mechanism and approaches for combining immunotherapy. Cancers (Basel). 2023;15(6):1619. 10.3390/cancers15061619.

Figures

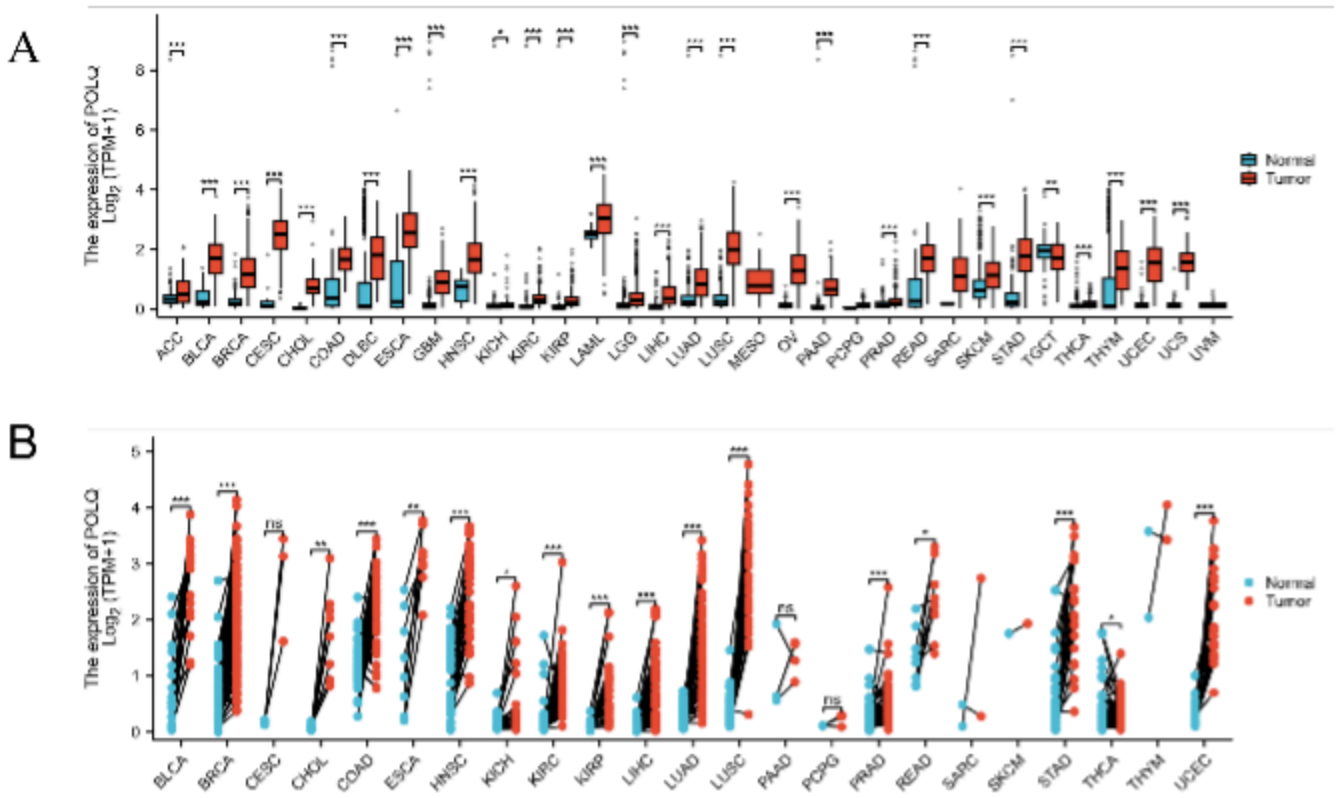


Figure 1

Expression of POLQ mRNA across pan-cancer cohorts. (A) Comparison of POLQ expression between tumor and normal tissues among 33 cancer types from the TCGA-GTEx combined dataset. Each dot represents an individual sample. (B) Paired expression analysis of POLQ in tumor and adjacent normal tissues across 23 cancer types from the TCGA dataset. Data are presented as mean ± s.d. Statistical significance markers: *P < 0.05, **P < 0.01, ***P < 0.001; ns, not significant.

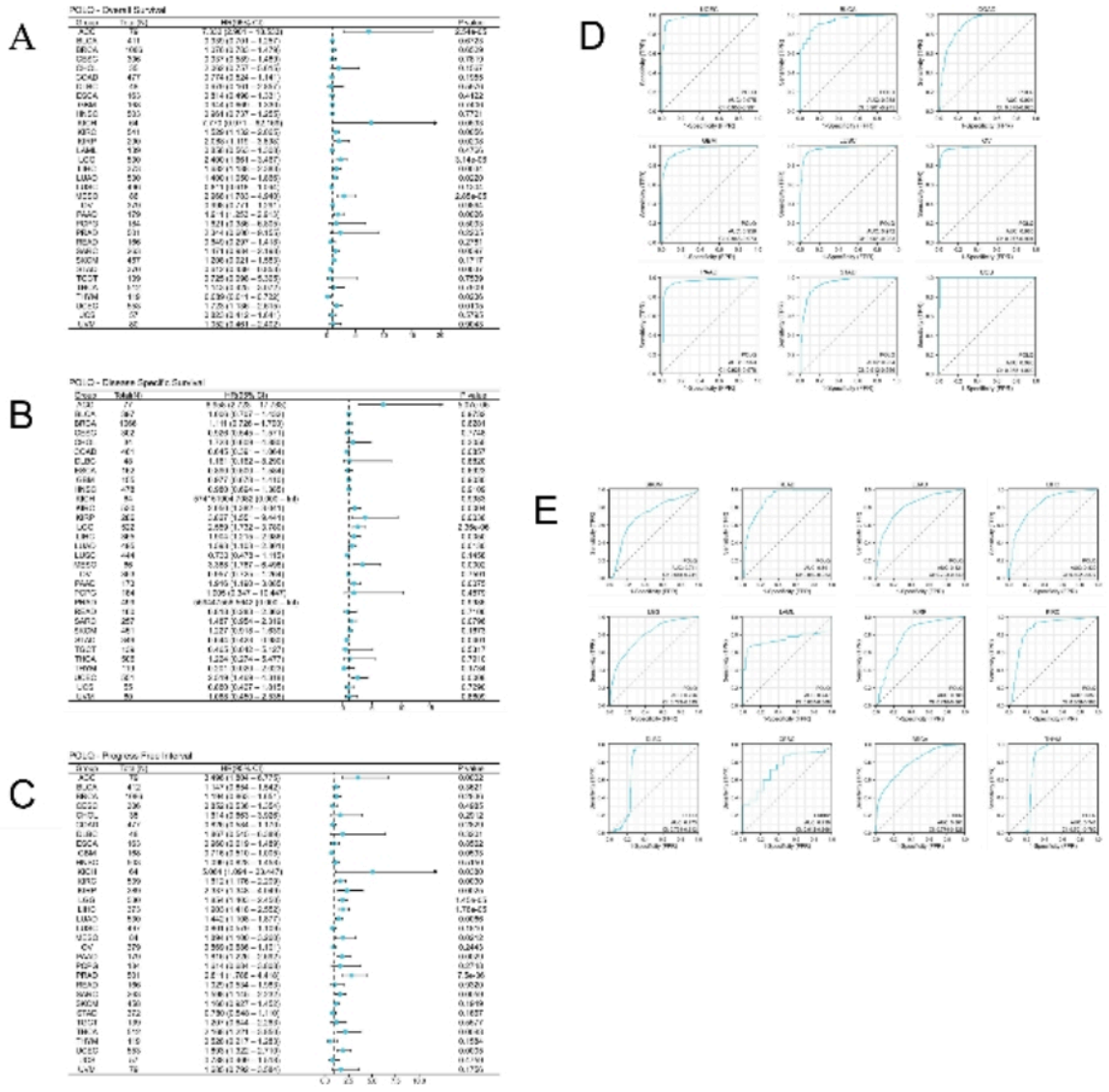


Figure 2

Prognostic and diagnostic analysis of POLQ across diverse cancers. (A–C) Forest plots visualizing associations between POLQ expression and OS (A), DSS (B) and PFI (C). (D–E) ROC curves assessing tumor versus normal diagnostic performance of POLQ for representative cancer types (UCEC, BLCA, COAD, GBM, LUSC, OV, STAD and PAAD).

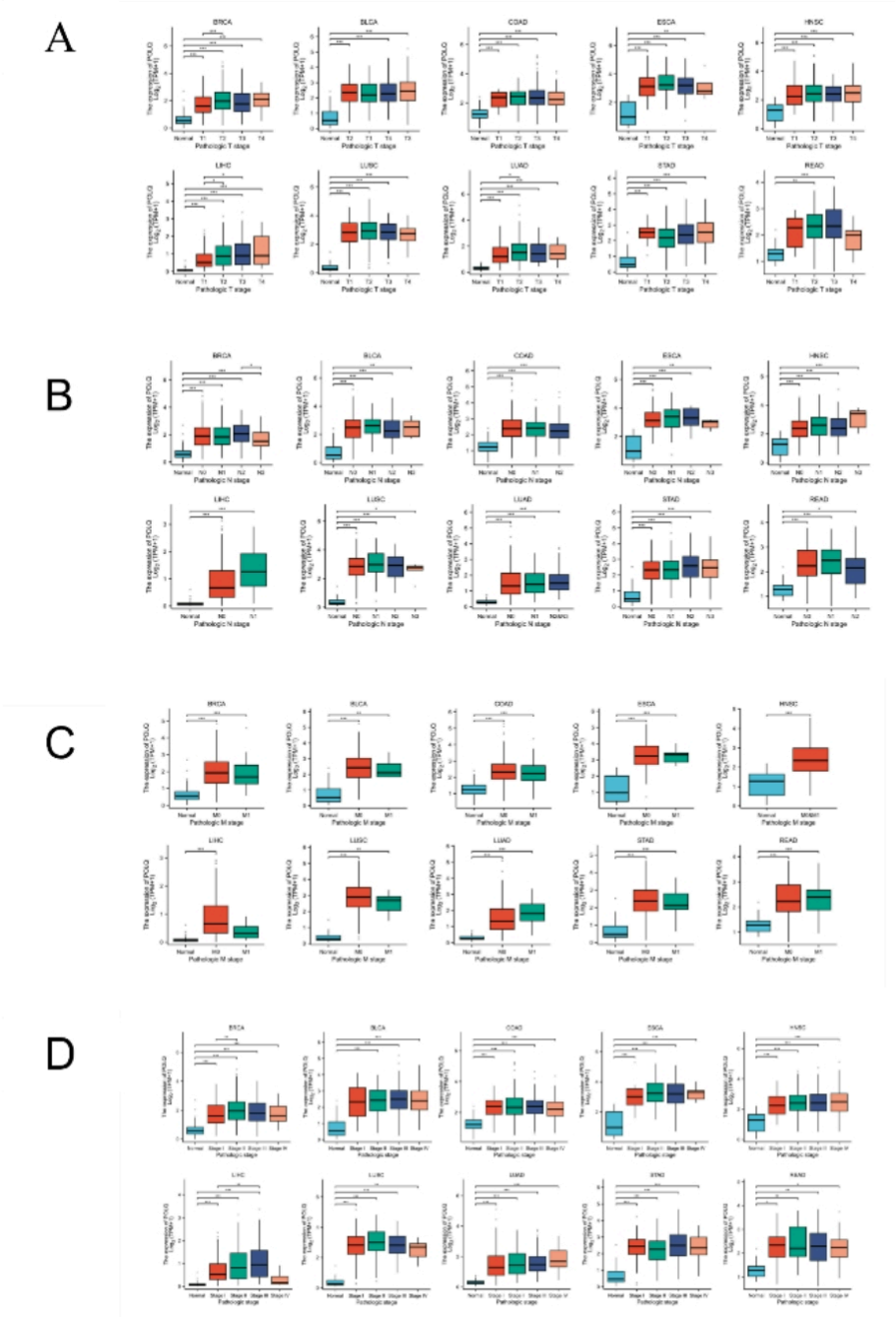


Figure 3

Pan-cancer POLQ expression across different clinicopathological stages. (A–D) POLQ expression grouped by T stage (A), N stage (B), M stage (C) and overall pathological stage (D) across ten cancer subtypes (BLCA, BRCA, COAD, ESCA, HNSC, LIHC, LUAD, LUSC, READ and STAD). Kruskal-Wallis test with Dunn's multiple comparison test and Benjamini-Hochberg adjustment was applied for intergroup comparisons.

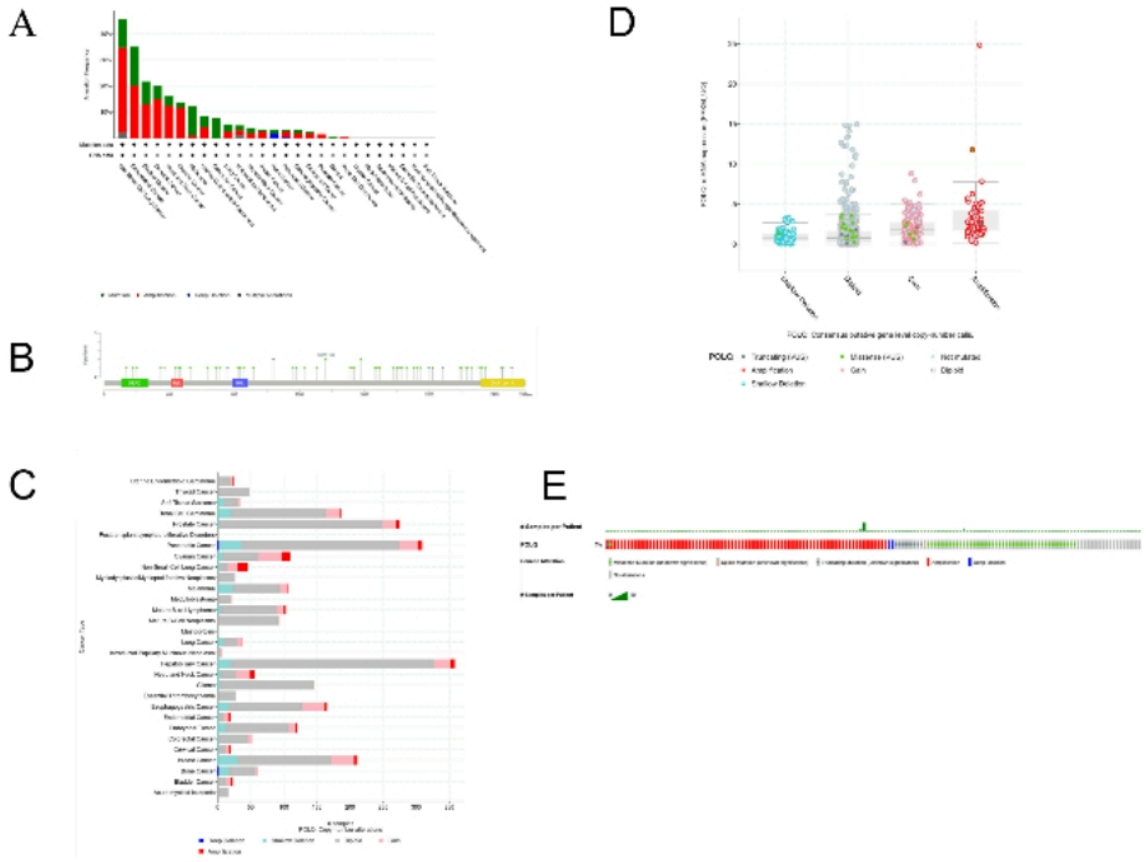


Figure 4

Pan-cancer genetic alteration landscape of POLQ. (A) Genetic alteration frequency summary across cancer types. (B) Mutation event distribution mapped onto POLQ protein functional domains. (C) Copy number variation event frequencies across cancer types. (D) POLQ mRNA expression stratified by copy number status. (E) Patient-level individual sample genetic alteration profiles. OncoPrint color coding: red = amplification; blue = deep deletion; green = missense mutation; black = truncating mutation.

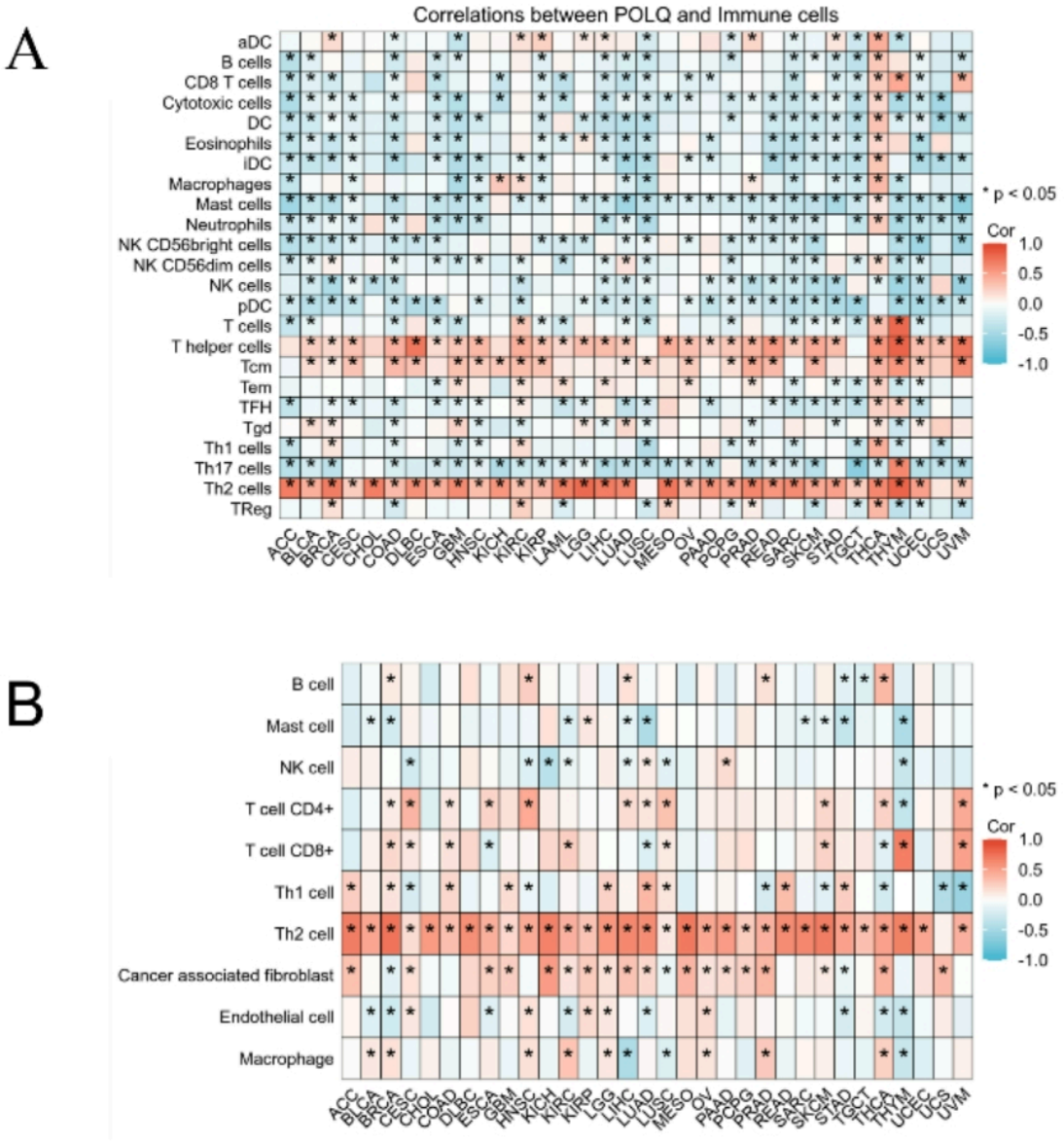


Figure 5

Immune cell infiltration estimates for pan-cancer cohorts. Immune cell infiltration levels across 33 cancer types computed using multiple algorithms (CIBERSORT and EPIC).

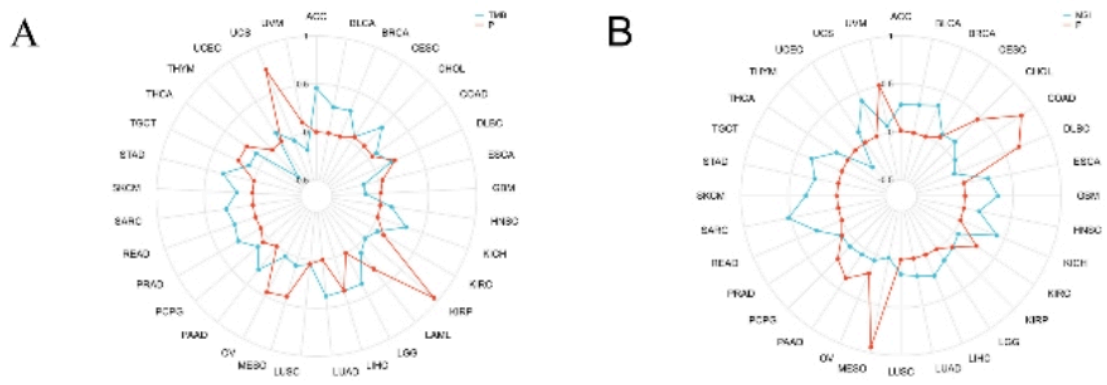


Figure 6

Radar plots for pan-cancer TMB and MSI correlation analysis. (A) Correlation coefficients between POLQ expression and TMB across cancer types. (B) Correlation coefficients between POLQ expression and MSI across cancer types.

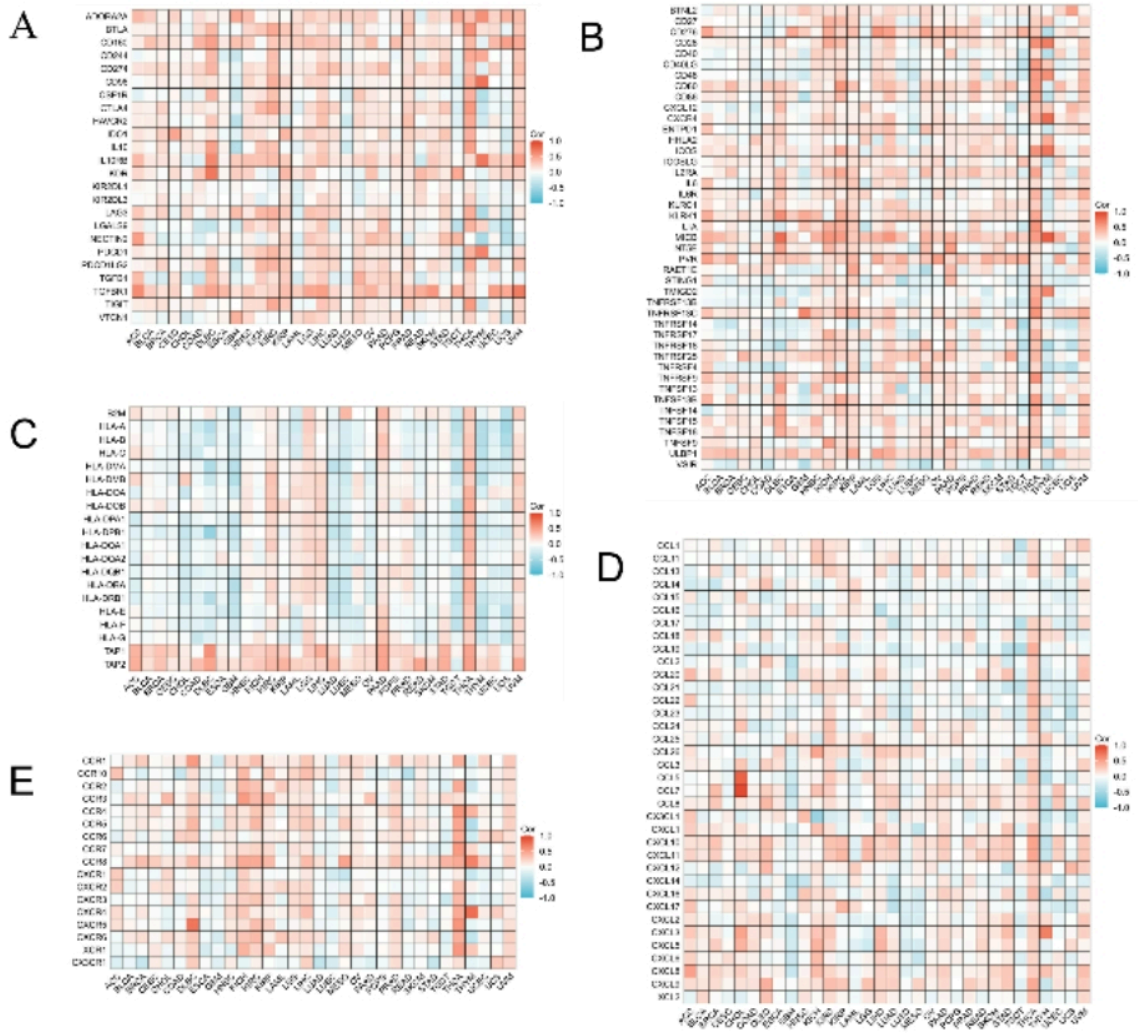


Figure 7

Correlation heatmaps of immune-relevant gene sets across pan-cancer cohorts. Color gradient denotes Spearman correlation coefficients ranging from −1.0 (blue) to 1.0 (red). (A) Immune suppressor gene correlation heatmap. (B) Immune activator gene correlation heatmap. (C) MHC and antigen presentation-related gene correlation heatmap. (D) Inflammatory factor gene correlation heatmap. (E) Inflammatory receptor gene correlation heatmap.

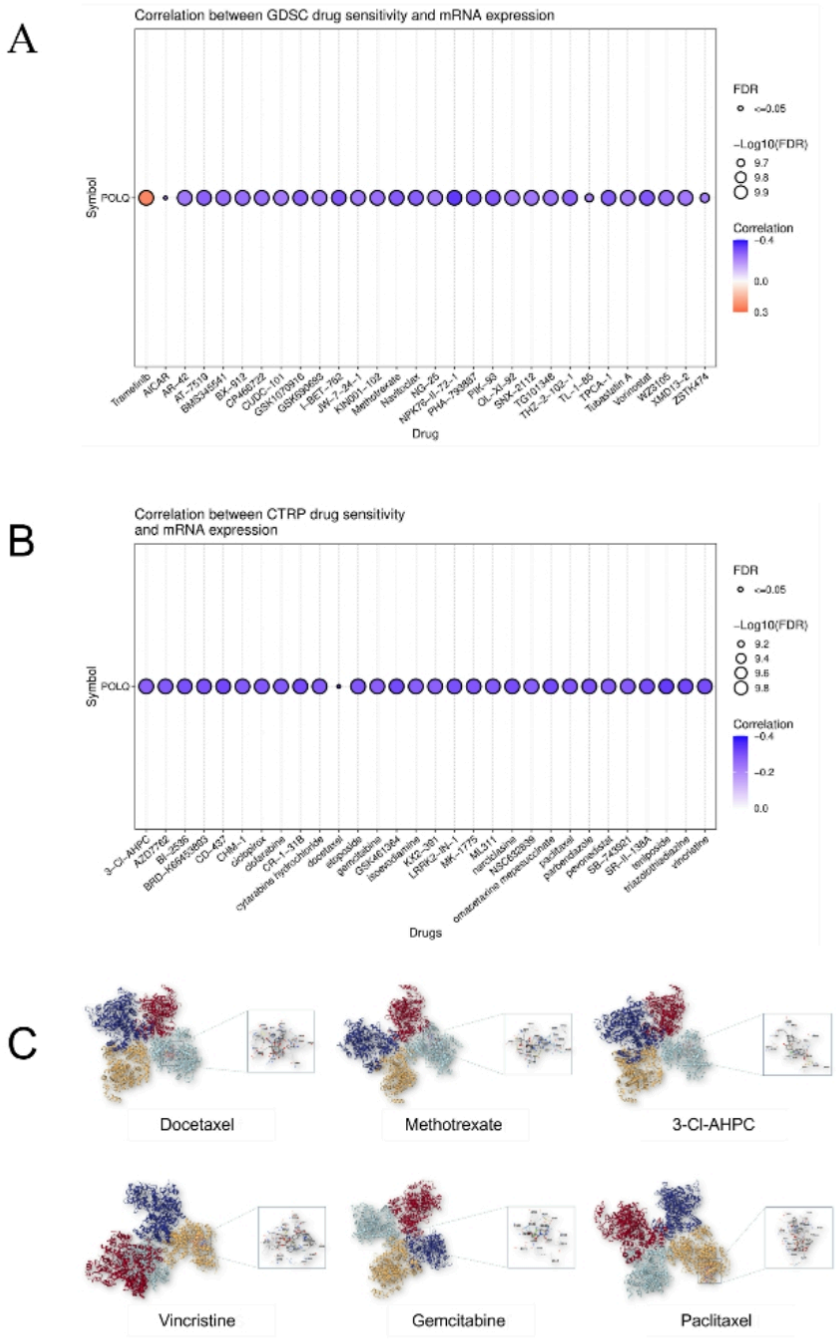


Figure 8

Pan-cancer drug sensitivity analysis and in silico molecular docking outputs for POLQ. (A) POLQ expression-drug sensitivity correlation derived from GDSC database. (B) POLQ expression-drug sensitivity correlation derived from CTRP database. FDR ≤ 0.05 was used as significance cutoff in panels A and B. (C) Calculated docking binding energies for six candidate small molecule compounds against POLQ protein; more negative values correspond to higher predicted binding affinity. Drug sensitivity

statistics were generated by GSCA platform. POLQ 3D structure was obtained from RCSB PDB; compound structures were retrieved from PubChem; blind docking simulation was completed on CB-Dock2 server.

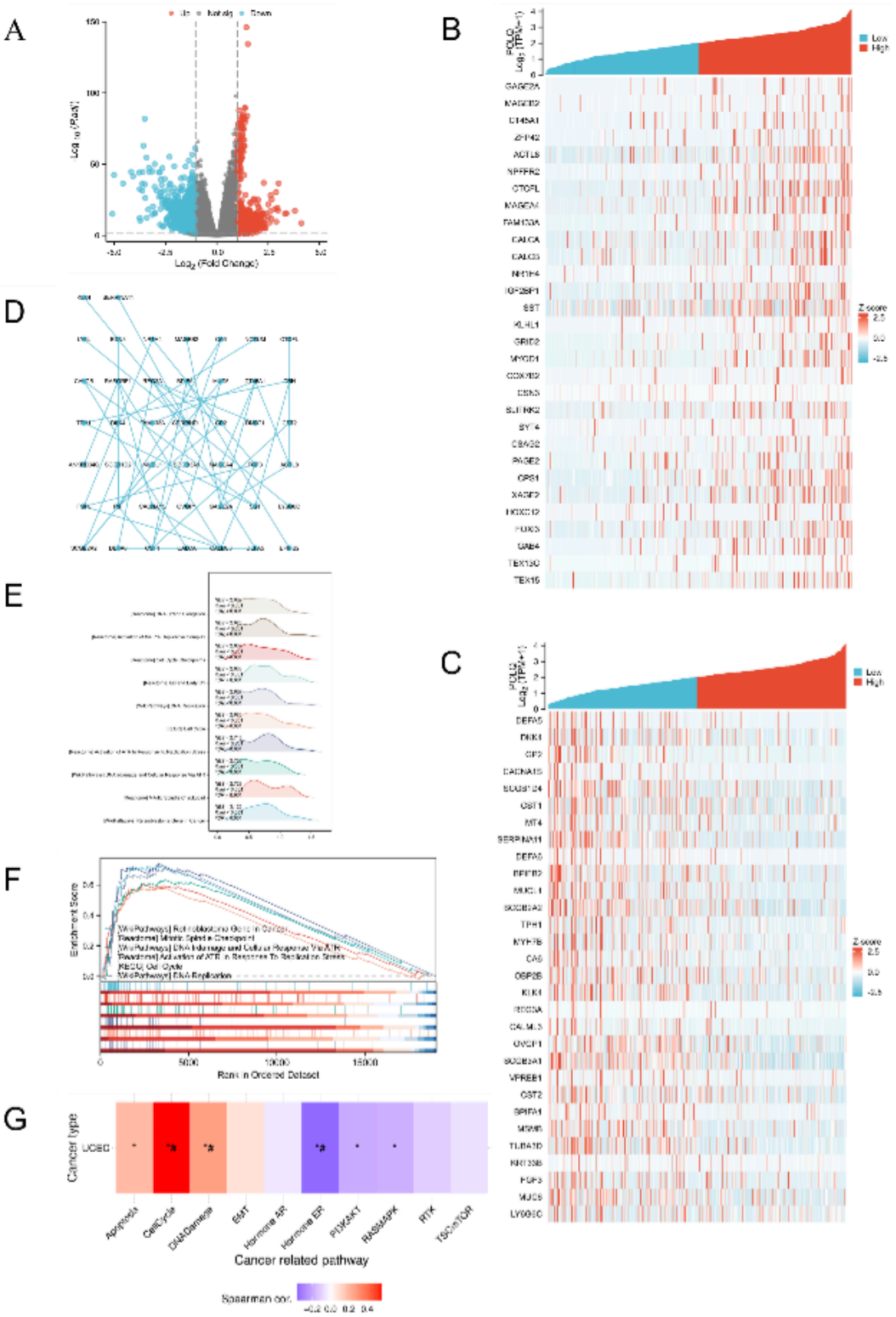


Figure 9

Differential gene expression and functional enrichment analyses for UCEC. (A) Volcano plot illustrating global DEG distribution between POLQ high and POLQ low subgroups; red: significantly upregulated genes; blue: significantly downregulated genes. (B) Co-expression heatmap for top 30 upregulated DEGs. (C) Co-expression heatmap for top 30 downregulated DEGs. (D) PPI interaction network constructed from identified DEGs. (E) GSEA ridge plot showing global functional pathway enrichment profiles. (F) Detailed visualization for selected core enriched GSEA pathways. (G) Correlation between POLQ and cancer-relevant signaling pathways analysed using GSCA database.

Supplementary Files

This is a list of supplementary files associated with this preprint. Click to download.

- Supplementary1.zip